Molecular Cell, Volume *77*

Supplemental Information

TFIIIC Binding to Alu Elements Controls Gene Expression via Chromatin Looping and Histone Acetylation

Roberto Ferrari, Lara Isabel de Llobet Cucalon, Chiara Di Vona, François Le Dilly, Enrique Vidal, Antonios Lioutas, Javier Quilez Oliete, Laura Jochem, Erin Cutts, Giorgio Dieci, Alessandro Vannini, Martin Teichmann, Susana de la Luna, and Miguel Beato

Fig. S1

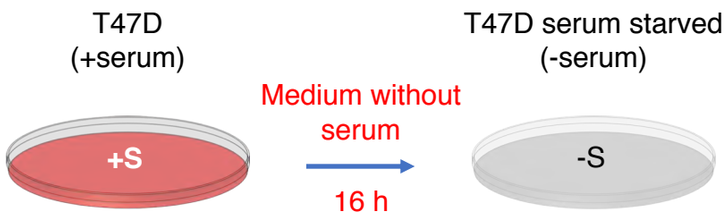
A
T47D
(+serum)
T47D serum starved
(-serum)
Medium without
serum
16 h
+S
-S

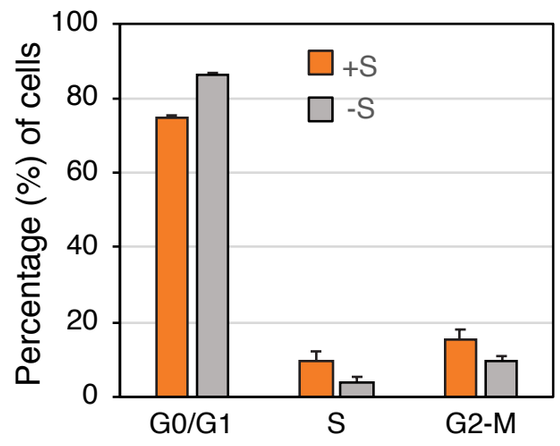
B
Percentage (%) of cells
100
80
60
40
20
0
+S
-S
G0/G1
S
G2-M

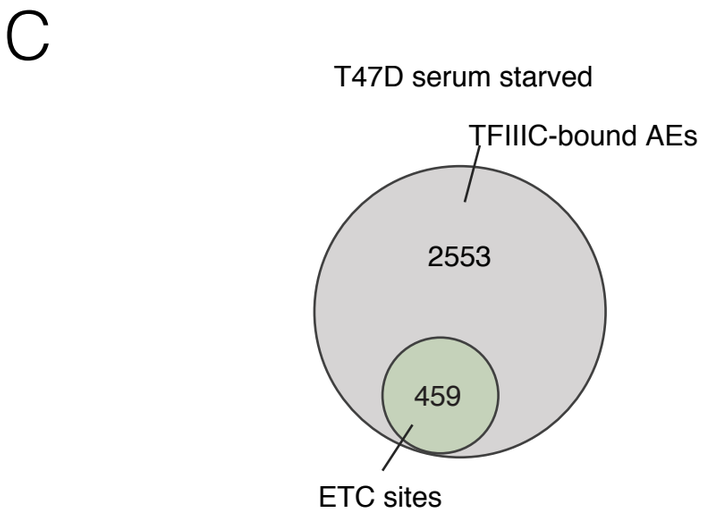
C
T47D serum starved
TFIIIC-bound AEs
2553
459
ETC sites

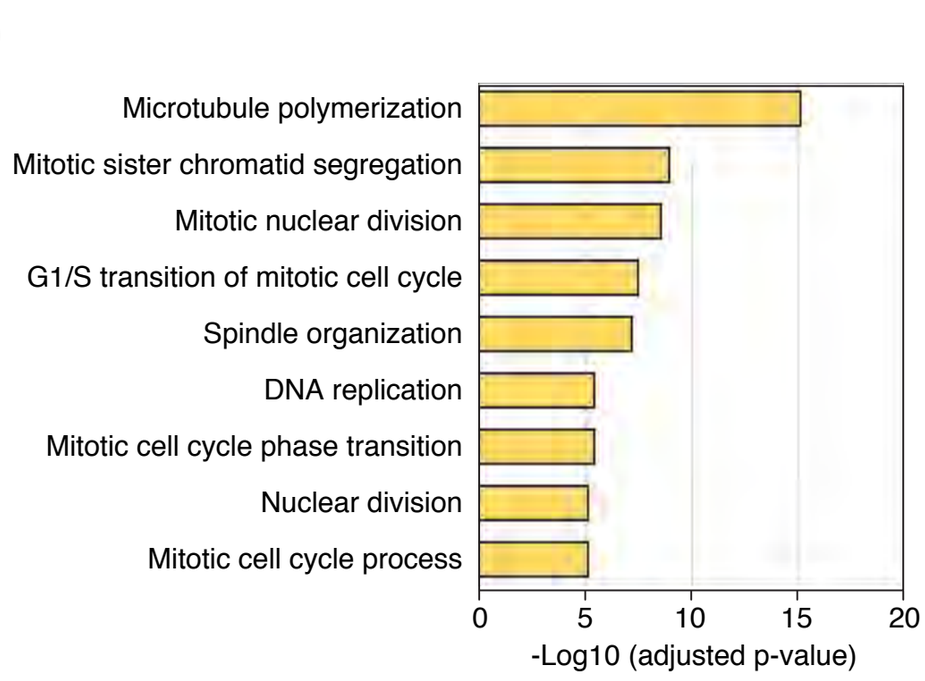
D
Microtubule polymerization
Mitotic sister chromatid segregation
Mitotic nuclear division
G1/S transition of mitotic cell cycle
Spindle organization
DNA replication
Mitotic cell cycle phase transition
Nuclear division
Mitotic cell cycle process
0
5
10
15
20
-Log10 (adjusted p-value)

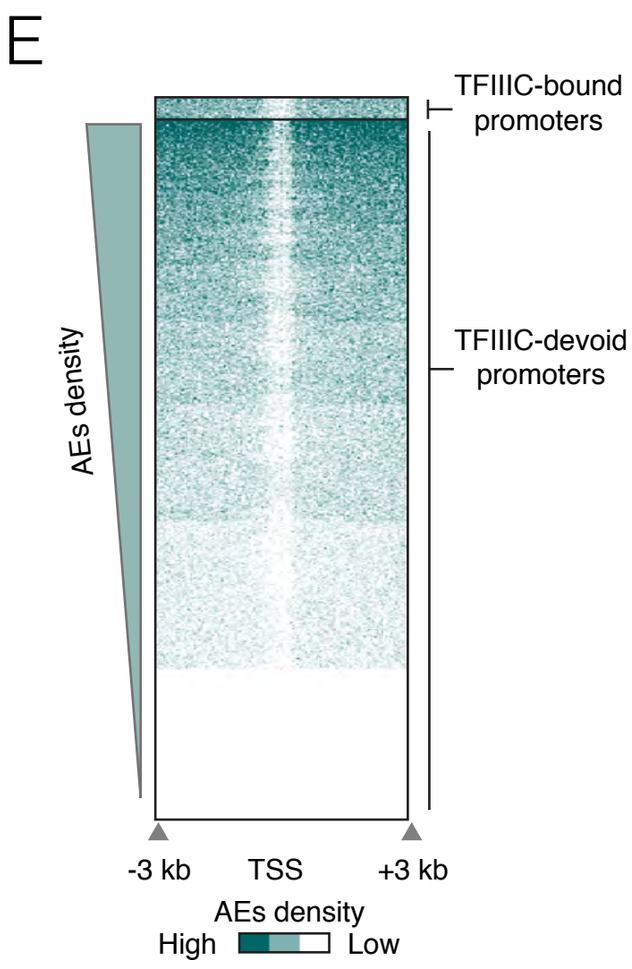
E
TFIIIC-bound
promoters
TFIIIC-devoid
promoters
AEs density
-3 kb
TSS
+3 kb
AEs density
High
Low

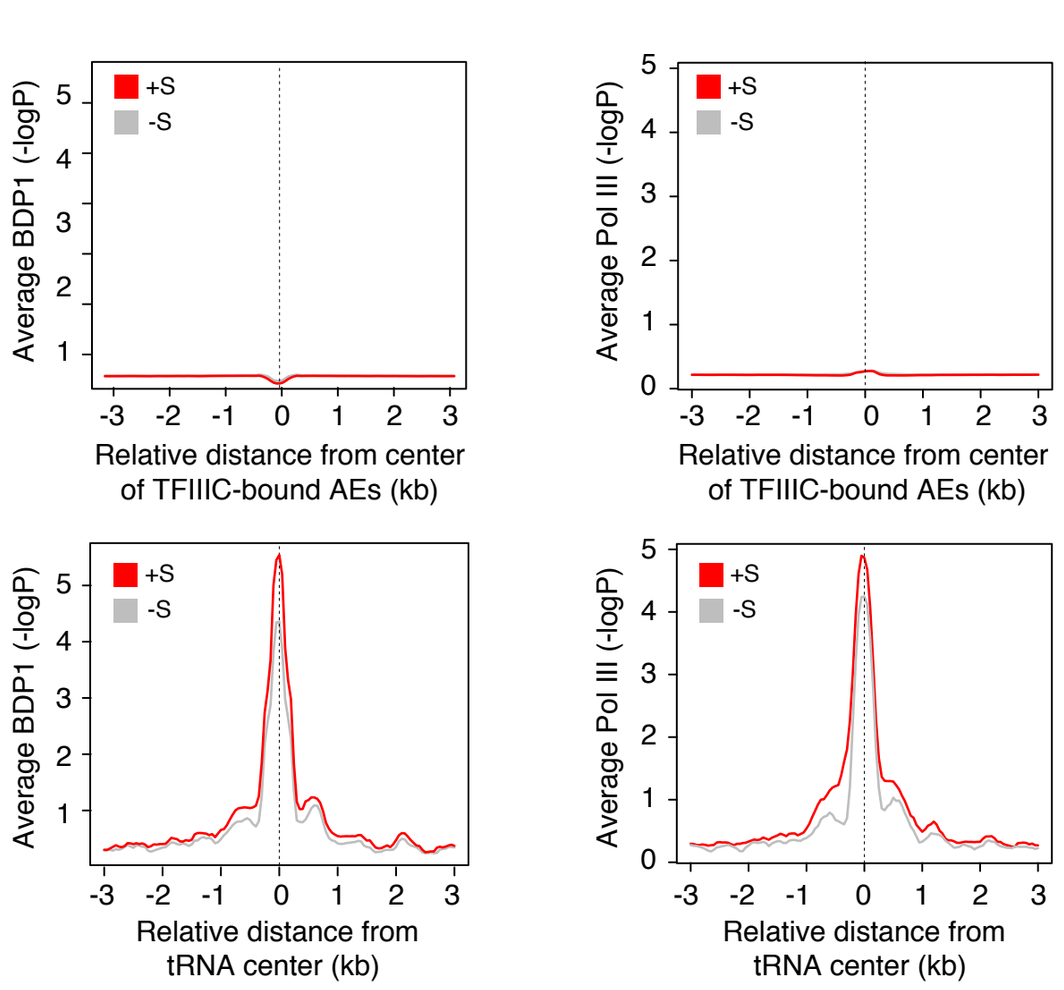
F
Average BDP1 (-logP)
Average Pol III (-logP)
+S
-S
Relative distance from center
of TFIIIC-bound AEs (kb)
Relative distance from
tRNA center (kb)

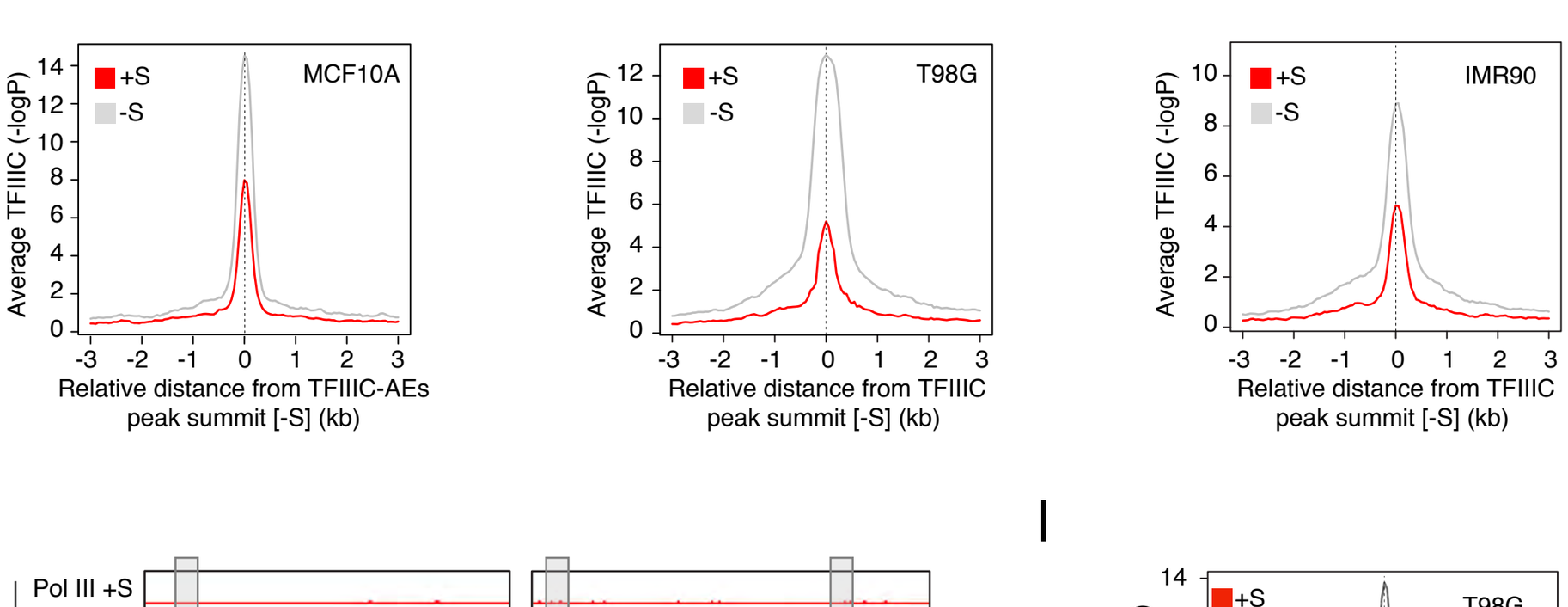
G
MCF10A
T98G
IMR90
Average TFIIIC (-logP)
+S
-S
Relative distance from TFIIIC-AEs
peak summit [-S] (kb)
Relative distance from TFIIIC
peak summit [-S] (kb)

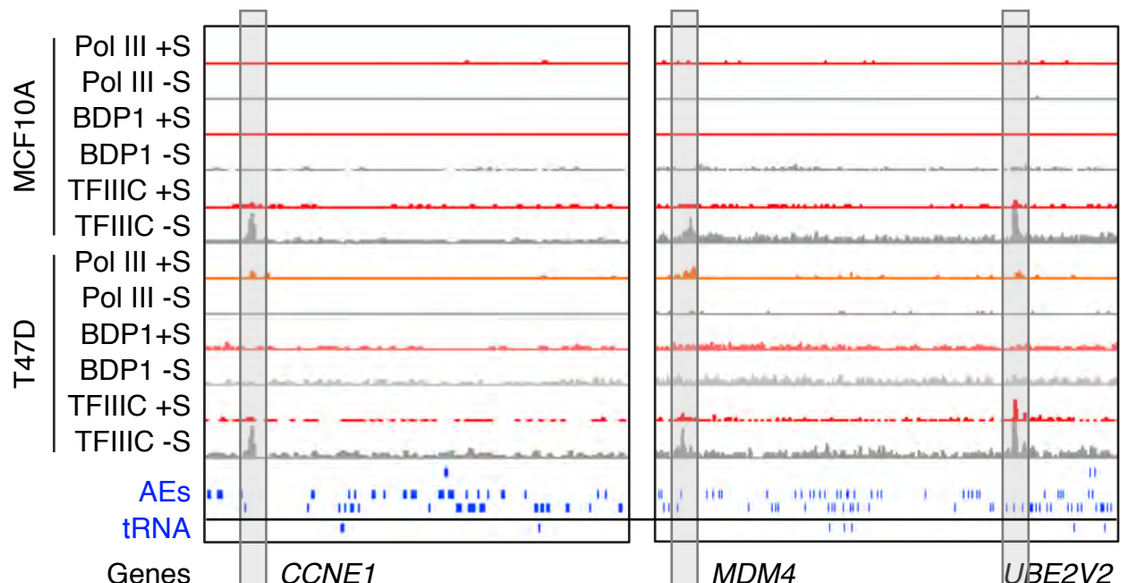
H
MCF10A
T47D
Pol III +S
Pol III -S
BDP1 +S
BDP1 -S
TFIIIC +S
TFIIIC -S
AEs
tRNA
Genes
CCNE1
MDM4
UBE2V2

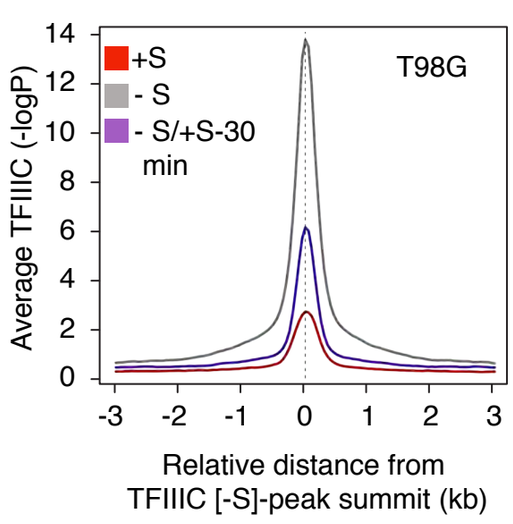
I
T98G
+S
- S
- S/+S-30
min
Average TFIIIC (-logP)
Relative distance from
TFIIIC [-S]-peak summit (kb)

Figure S1. Tumorigenic and normal cell lines show TFIIIC (but not TFIIIB nor Pol III) binding to AEs close to Pol II promoters of cell cycle-related genes upon serum starvation (SS), related to Figure 1.

(**A**) Schematic view of the experimental design.

(**B**) Cell cycle profile of T47D cells grown in normal conditions (+S, orange) or upon 16 h of SS (–S grey). Note that T47D cells show a cell cycle profile highly enriched in the G1 population in the normal growth conditions; although a slight increase in the proportion of cells in G1 phase with a concomitant reduction in the S and G2/M phases was detected following serum depletion, it was not statistically significant (Chi-square test, p-value = 0.09).

(**C**) Proportional Venn diagram of total AEs bound by TFIIIC detected *vs* those containing ETC sites (with only B-box) in the serum-starved cells.

(**D**) Bar plots of gene ontology (GO) enrichment for Pol II genes with TFIIIC-bound within 5 kb of their TSSs) in the serum-starved cells. GO terms were calculated by DAVID (Molecular Function and Biological Processes combined) and ranked from the lowest to the highest p-value of the first nine terms found.

(**E**) Heatmap of AEs density across all human TSSs spanning a 6 kb-region and sorted by high to low AEs density. TFIIIC-associated promoters are shown at the top. Color bar scale with increasing shades of color stands for higher AEs density.

(**F)** CEAS plots of the average binding to AEs bound by TFIIIC (top panels) or to tDNAs bound by TFIIIC (bottom panels) for BDP1 (left) and Pol III/RPC39 (right) in T47D grown in normal condition (+S, red) or upon SS (-S, grey) (plotted is the –log10 of the Poisson p-value).

(**G**) CEAS plots of TFIIIC average binding for MCF10A, T98G and IMR90 cells in normal growth conditions (+S, red) and following SS (–S, grey, see Methods for specific conditions for each cell line). The graphs are plotted over the summit of TFIIIC peaks in the –S condition (plotted is the –log10 of the Poisson p-value). The enrichment in peaks corresponds to AEs (not shown).

(**H**) Genome browser view of *CCNE1, MDM4 and UBE2V2* loci with ChIP-seq data for Pol III, BDP1 and TFIIIC in MCF10A and T47D breast cell lines. The graph includes the tracks for AEs and tDNAs. Highlighted in grey is the AE bound by TFIIIC close to the TSS of the indicated genes and arrow shows direction of transcription.

(**I**) CEAS plot of TFIIIC average enrichment for T98G cells grown in normal conditions (+S, red), SS (–S, grey), or SS followed by serum addition for 30 min (–S/+S-30 min, purple). The graphs are plotted over TFIIIC-peaks summit in the –S condition (plotted is the –log10 of the Poisson p-value).

Fig. S2

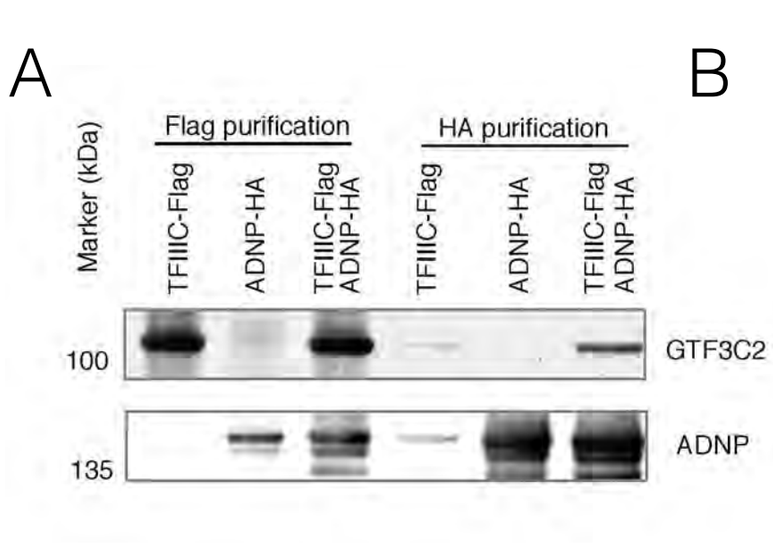
A
Flag purification
HA purification
Marker (kDa)
TFIIIC-Flag
ADNP-HA
TFIIIC-Flag ADNP-HA
TFIIIC-Flag
ADNP-HA
TFIIIC-Flag ADNP-HA
100
GTF3C2
135
ADNP

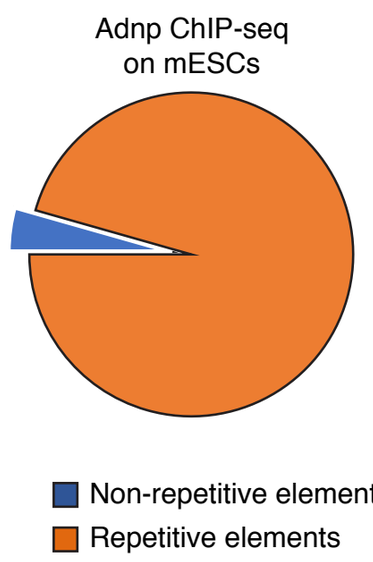
B
Adnp ChIP-seq on mESCs
Non-repetitive elements
Repetitive elements

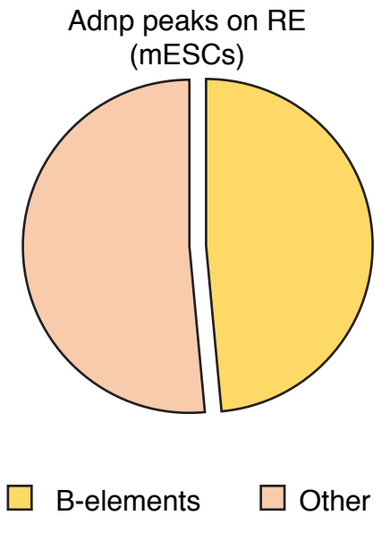
C
Adnp peaks on RE (mESCs)
B-elements
Other

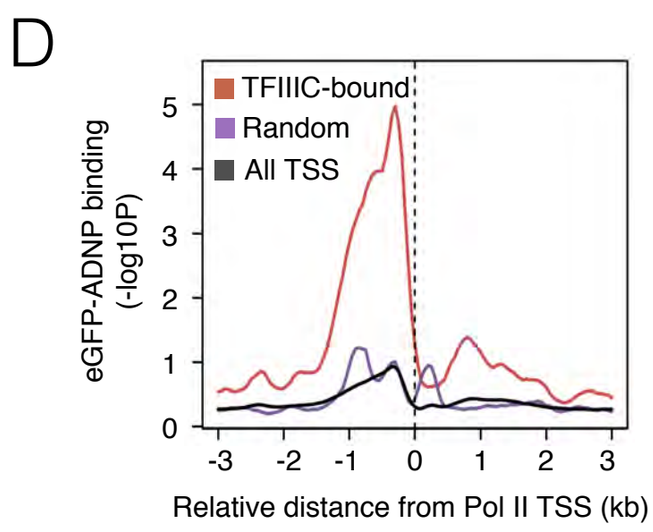
D
TFIIIC-bound
Random
All TSS
eGFP-ADNP binding (-log10P)
Relative distance from Pol II TSS (kb)

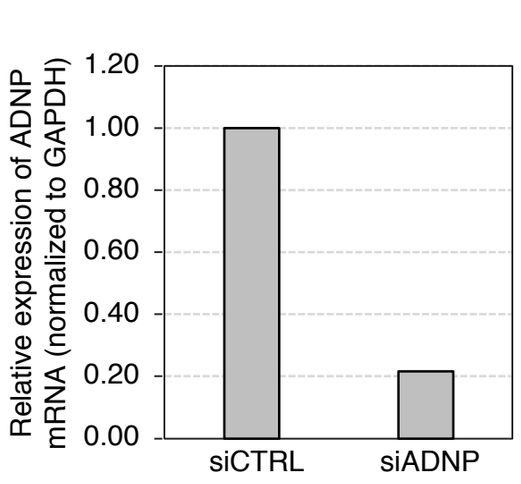
E
Relative expression of ADNP mRNA (normalized to GAPDH)
siCTRL
siADNP

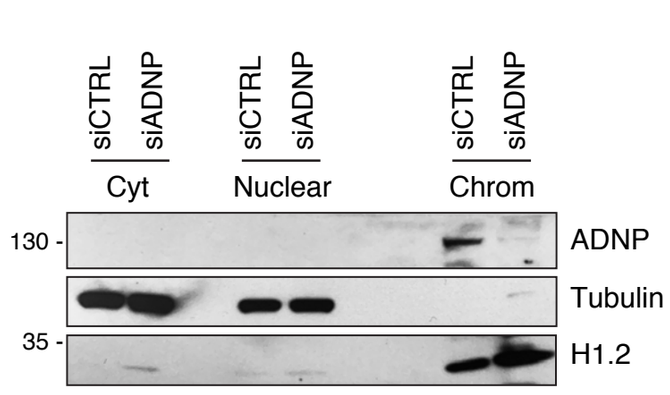
F
siCTRL
siADNP
Cyt
Nuclear
Chrom
130
ADNP
Tubulin
35
H1.2

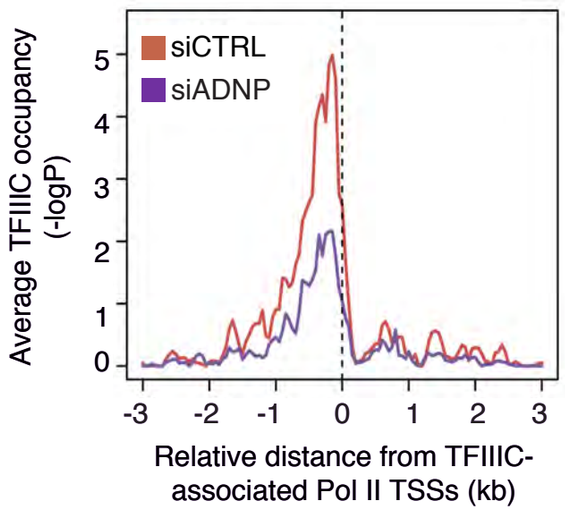
G
siCTRL
siADNP
Average TFIIIC occupancy (-logP)
Relative distance from TFIIIC-associated Pol II TSSs (kb)

Figure S2. ADNP depletion causes TFIIIC loss from TFIIIC-associated promoters upon serum starvation, Related to Figure 2.

(A) Western Blot analysis of tagged-immunopurification of TFIIIC and ADNP complexes as described in Figure 2B. FLAG- and HA-purified complexes were probed for the presence of TFIIIC (GTF3C2 subunit) and ADNP.

(**B**) Pie chart showing the percentage of mouse Adnp peaks found in mESCs belonging to repetitive elements and non-repetitive elements (analysis from GSE97945). Notice that almost all the binding of this factor lays on repetitive elements.

(**C**) Pie chart showing the percentage of Adnp peaks mapping to repetitive elements and belonging to B-elements or to other type of repetitive elements. Notice that more than 50% of Adnp peaks mapping to repetitive elements lay on B-elements.

(**D**) Average plot for ADNP-eGFP (GSE105573) enrichment across TFIIIC-associated Pol II promoters (red) spanning a 6 kb-region. The profile of a random set of genes of the same size (purple), as well as the average for all human TSSs (black) is also shown.

(**E**) qRT-PCR expression analysis of *ADNP* in serum-starved T47D cells (siCTRL and siADNP) corresponding to the experiment in Figure 2D. The value in siCTRL cells was arbitrarily set as 1. Note that the knockdown of *ADNP* reaches values almost 80% of its control.

(**F**) Immunoblot probing the levels of ADNP protein across three cellular fractions: cytoplasm (Cyt), nucleoplasm (Nuclear) and chromatin (Chrom) in serum-starved T47D cells transfected with siADNP or control siCTRL. Note that the largest pool of ADNP is found in the chromatin fraction and is strongly reduced upon knock down. α-Tubulin and histone H1.2 are used as controls for the subcellular fractionation.

(**G**) CEAS profile of TFIIIC enrichment over TFIIIC-associated Pol II promoters upon depletion of ADNP (siADNP, purple) compared to control cells (siCTRL, red) in serum-starved T47D. Note the strong reduction in TFIIIC occupancy (from -logP ~ 5 to -logP ~ 2.5) in ADNP knocked down cells.

Fig. S3

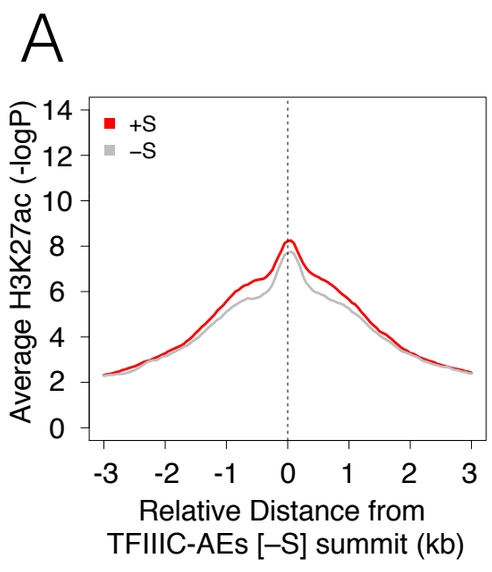
A
Average H3K27ac (-logP)
+S
–S
Relative Distance from
TFIIIC-AEs [–S] summit (kb)

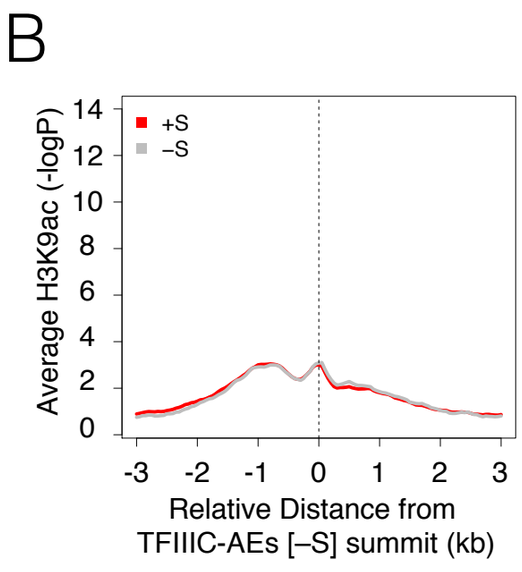
B
Average H3K9ac (-logP)
+S
–S
Relative Distance from
TFIIIC-AEs [–S] summit (kb)

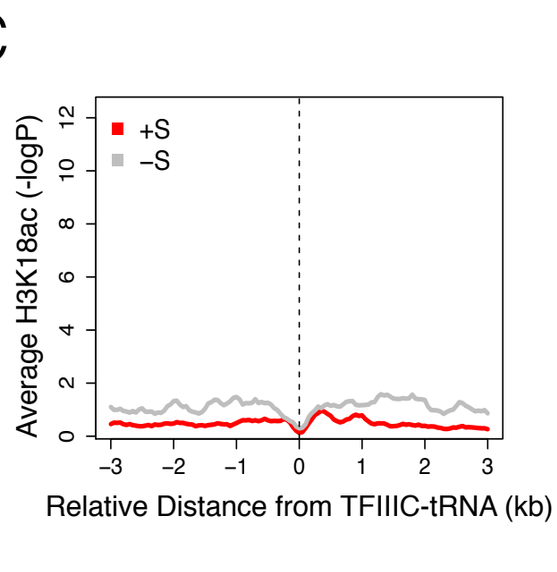
C
Average H3K18ac (-logP)
+S
–S
Relative Distance from TFIIIC-tRNA (kb)

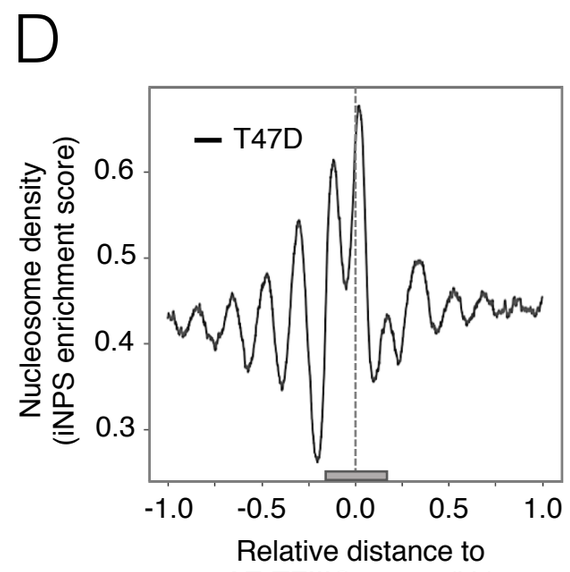
D
T47D
Nucleosome density
(iNPS enrichment score)
Relative distance to
AE-TFIIIC center (kb)

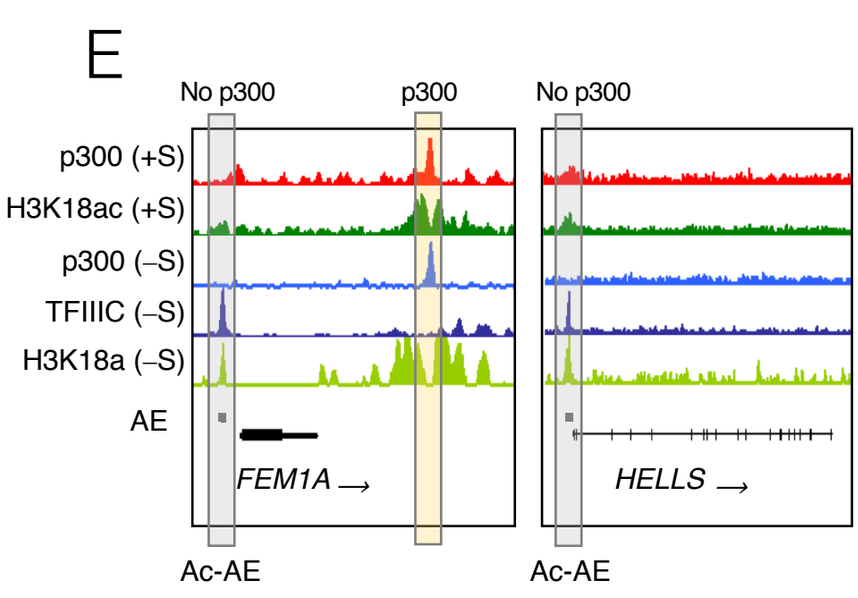
E
No p300
p300
No p300
p300 (+S)
H3K18ac (+S)
p300 (–S)
TFIIIC (–S)
H3K18a (–S)
AE
FEM1A
HELLS
Ac-AE
Ac-AE

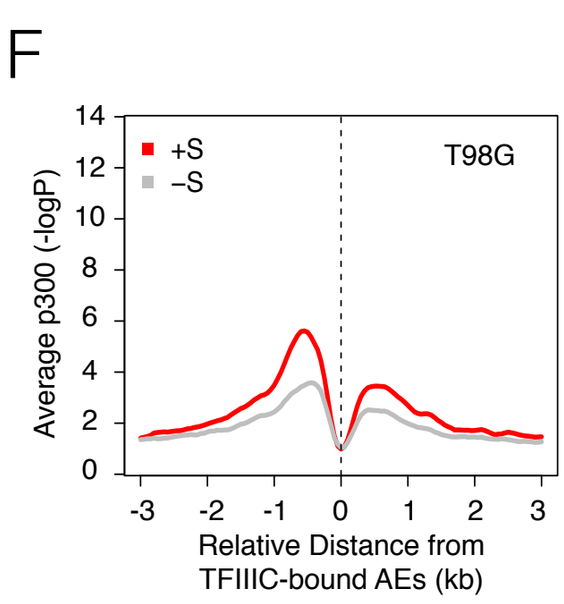
F
Average p300 (-logP)
+S
–S
T98G
Relative Distance from
TFIIIC-bound AEs (kb)

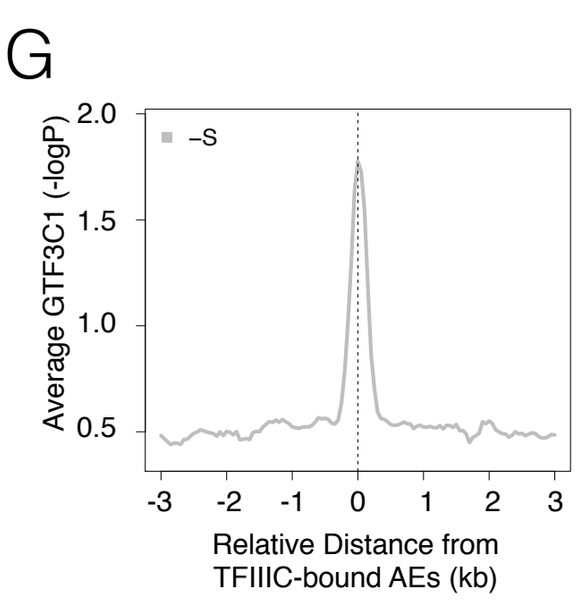
G
Average GTF3C1 (-logP)
–S
Relative Distance from
TFIIIC-bound AEs (kb)

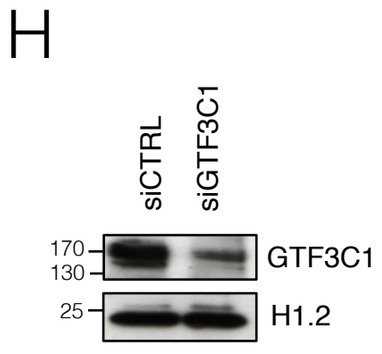
H
siCTRL
siGTF3C1
170
130
GTF3C1
25
H1.2

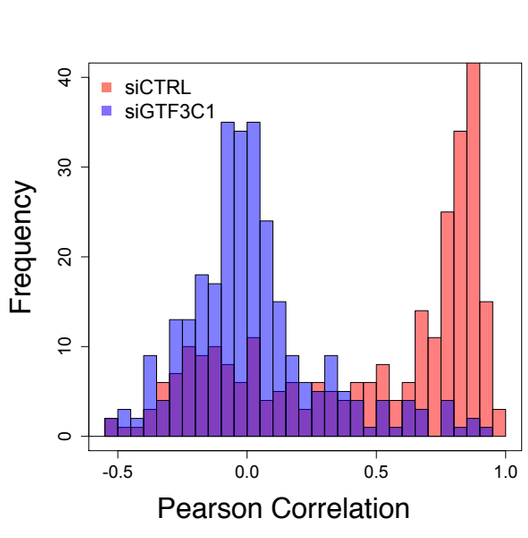
I
siCTRL
siGTF3C1
Frequency
Pearson Correlation

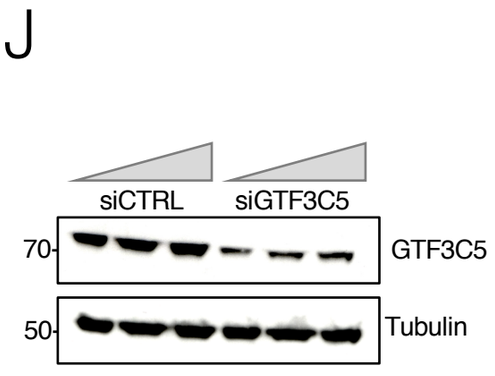
J
siCTRL
siGTF3C5
70
GTF3C5
50
Tubulin

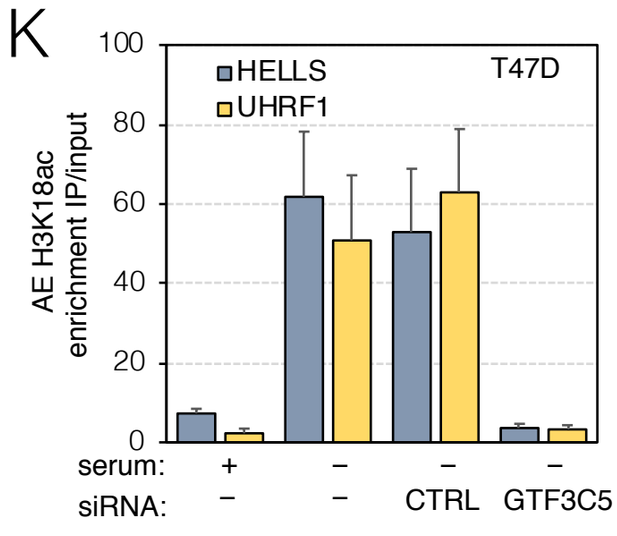
K
HELLS
UHRF1
T47D
AE H3K18ac
enrichment IP/input
serum:
siRNA:
CTRL
GTF3C5

Figure S3. Both H3K18ac and H3K27ac mark AEs occupied by TFIIIC, but only H3K18ac is changed upon serum starvation, Related to Figure 3.

(**A**) Sitepro profile of H3K27ac enrichment in T47D grown in the presence (+S, red) or absence of serum (–S, grey) over TFIIIC-bound AEs (plotted is the –log10 of the Poisson p-value). Note that the H3K27ac levels at these sites are independent of the growth conditions.

(**B**) Sitepro profile of H3K9ac enrichment in T47D grown in the presence (+S, red) or absence of serum (–S, grey) over TFIIIC-bound AEs (plotted is the –log10 of the Poisson p-value). Note the low levels of H3K9ac at these sites and their independence of the growth conditions.

(**C**) Sitepro profile of H3K18ac enrichment in T47D grown in the presence (+S, red) or absence (–S, grey) of serum at tDNAs (plotted is the –log10 of the Poisson p-value).

(**D**) Nucleosome density as mapped by MNase digestion across all TFIIIC-bound AEs in T47D cells using the iNPS score. The plot has been produced using NucMap (Zhao et al., 2019). Note the presence of at least one nucleosome over the region of the AE (represented as a grey rectangle).

(**E**) Genome browser view of representative TFIIIC-associated genes *FEM1A* and *HELLS* with ChIP-seq data for p300 and H3K18ac in T47D in the presence (+S) or absence (-S) of serum. The AE bound by TFIIIC in each locus is shown by a grey rectangle. The gene structure and the direction of transcription (arrow) are shown at the bottom. Note that p300 is not recruited at the AEs bound by TFIIIC (grey boxes) as it is for other adjacent intergenic regions (yellow box).

(**F**) Average plot for p300 occupancy across all TFIIIC-bound AEs spanning a 6 kb-region in T98G grown in the presence (+S, red) or absence (-S, grey) of serum. Data was from GSE21026.

(**G**) Average plot for GTF3C1 occupancy across all TFIIIC-bound AEs spanning a 6 kb-region in T47D grown in the absence of serum.

(**H**) Immunoblot probing GTF3C1 protein levels in serum-starved T47D cells transfected with siGTF3C1 or siCTRL as in Figure 3H. Histone H1.2 is shown as loading control.

(**I**) Histogram plot of Pearson's correlation frequencies of H3K18ac colocalization with DAPI staining of Figure 3H. The large majority of cells in T47D siCTRL cells had H3K18ac colocalizing with DAPI, whereas cellular ablation of GTF3C1 caused the loss of H3K18ac and consequently its colocalization with DAPI.

(**J**) Immunoblot probing GTF3C5 protein levels in T47D cells transfected with increasing concentration of siGTF3C5 or control siCTRL.

(**K**) ChIP-qPCR showing loss of H3K18ac enrichment at two AEs bound by TFIIIC (*UHRF1* and *HELLS* loci) in serum-starved T47D upon knock down of *GTF3C5* by siRNA. The graph shows mean and SD of 2 independent experiments. Depletion levels are shown in Figure S3J.

Fig. S4

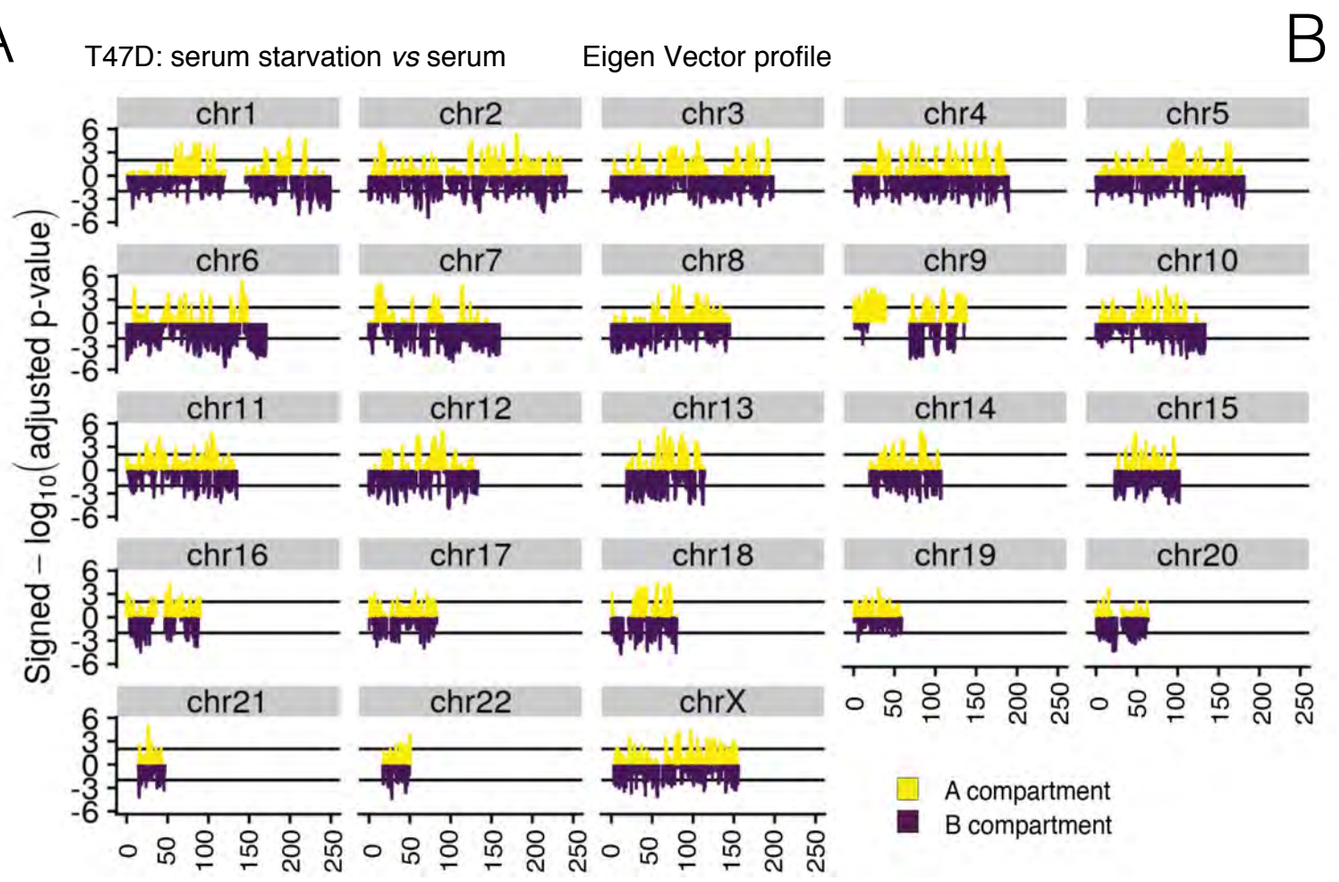
A
T47D: serum starvation vs serum
Eigen Vector profile
chr1
chr2
chr3
chr4
chr5
chr6
chr7
chr8
chr9
chr10
chr11
chr12
chr13
chr14
chr15
chr16
chr17
chr18
chr19
chr20
chr21
chr22
chrX
Signed − log10(adjusted p-value)
0
50
100
150
200
250
A compartment
B compartment

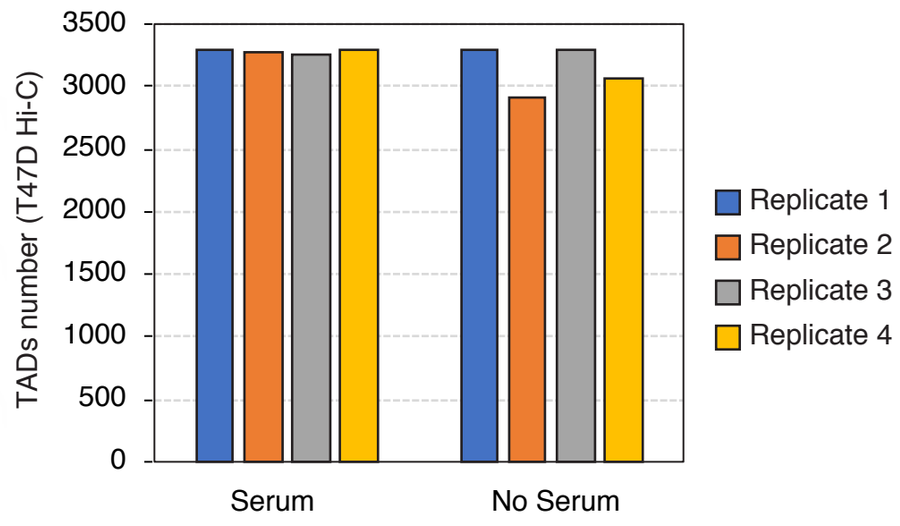
B
TADs number (T47D Hi-C)
3500
3000
2500
2000
1500
1000
500
0
Serum
No Serum
Replicate 1
Replicate 2
Replicate 3
Replicate 4

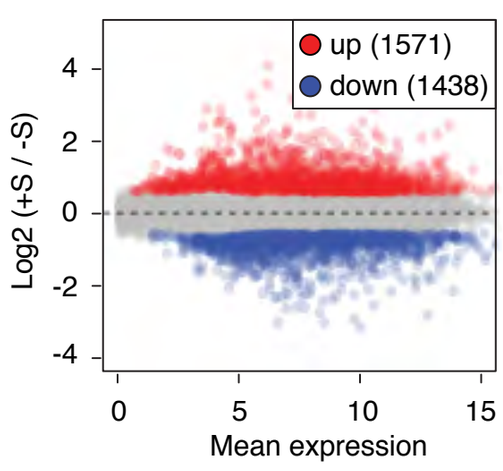
C
up (1571)
down (1438)
Log2 (+S / -S)
Mean expression

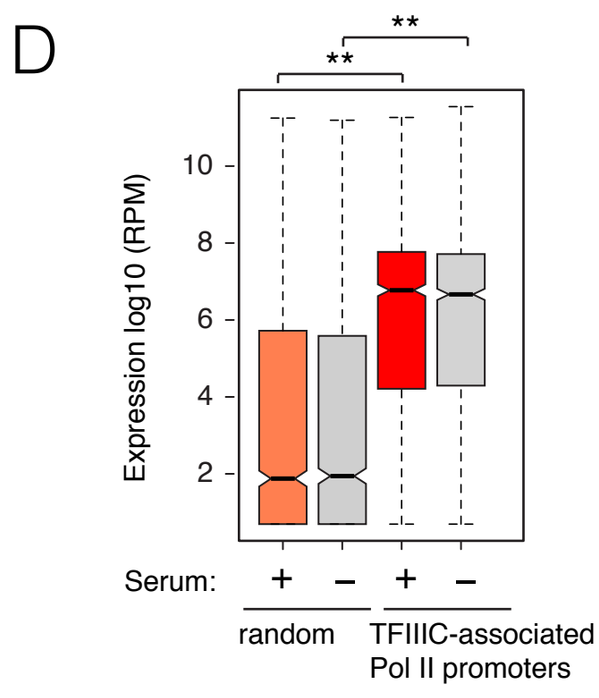
D
**
**
Expression log10 (RPM)
Serum:
+
−
+
−
random
TFIIIC-associated
Pol II promoters

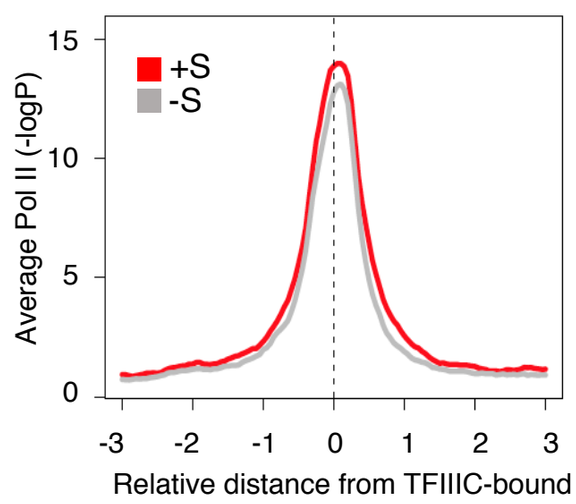
E
+S
-S
Average Pol II (-logP)
Relative distance from TFIIIC-bound
Pol II promoters (kb)

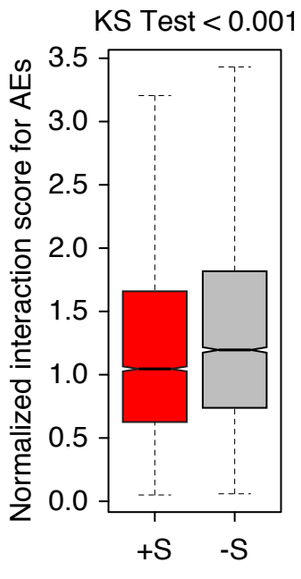
F
KS Test < 0.001
Normalized interaction score for AEs
+S
-S

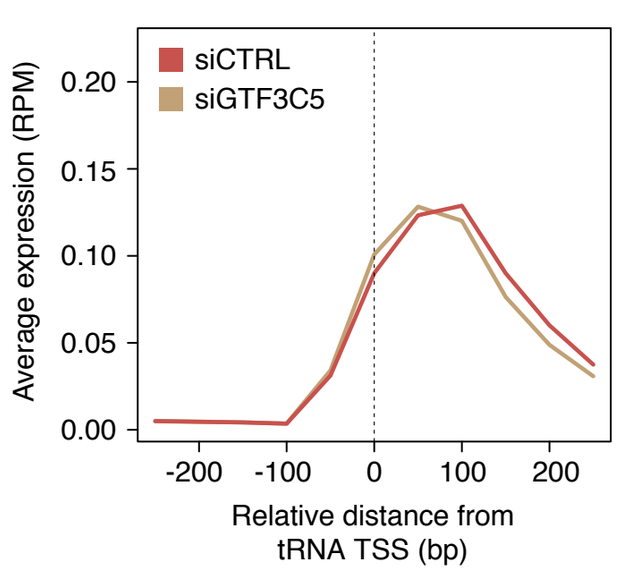
G
siCTRL
siGTF3C5
Average expression (RPM)
Relative distance from
tRNA TSS (bp)

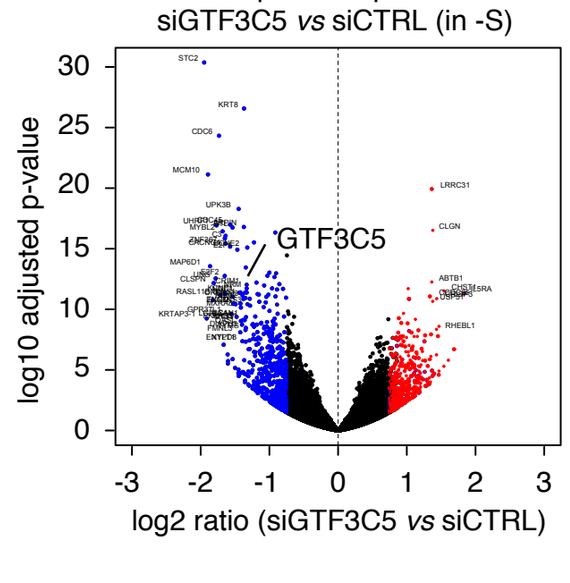
H
Gene expression profile T47D
siGTF3C5 vs siCTRL (in -S)
GTF3C5
log10 adjusted p-value
log2 ratio (siGTF3C5 vs siCTRL)

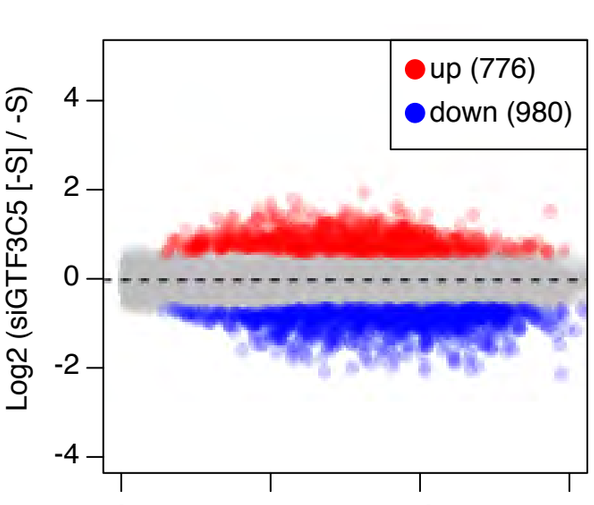
I
up (776)
down (980)
Log2 (siGTF3C5 [-S] / -S)
Mean across treatment

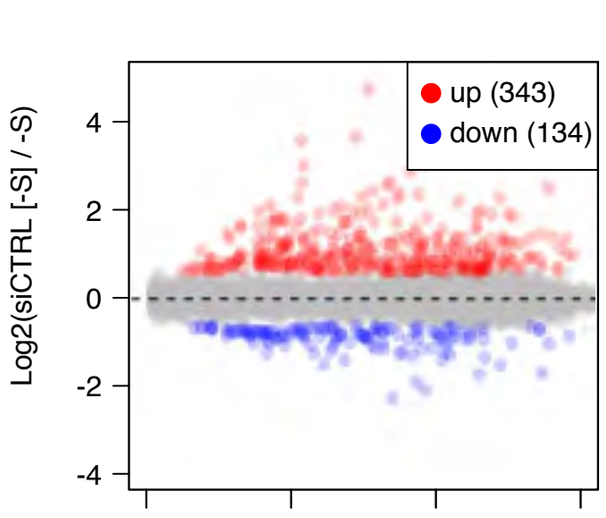
J
up (343)
down (134)
Log2(siCTRL [-S] / -S)
Mean across treatment

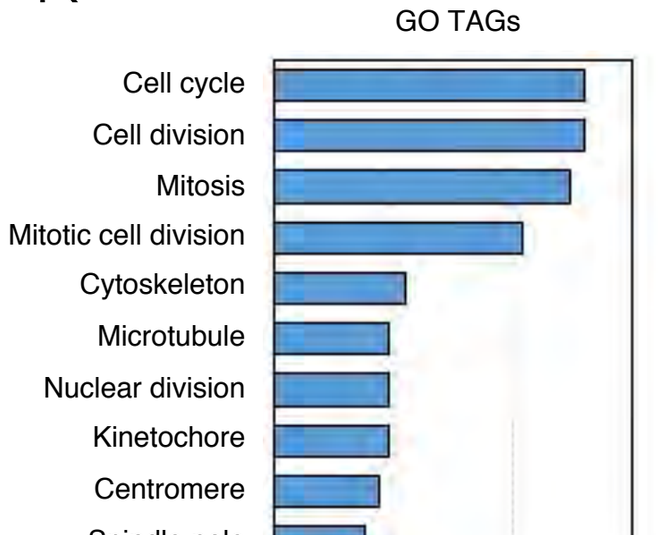
K
GO TAGs
Cell cycle
Cell division
Mitosis
Mitotic cell division
Cytoskeleton
Microtubule
Nuclear division
Kinetochore
Centromere
Spindle pole
-Log10 (adjusted p-value)

L
G1
S
G2/M
Percentage of cells
−S
siCTRL
siGTF3C5
*
*

Figure S4. Global gene expression analysis in T47D grown in normal conditions and after serum deprivation and dependence on TFIIIC, Related to Figure 4.

(**A**) Eigen Vector profile (-log10 adjusted p-value) for changes in A and B compartments in Hi-C experiments (4 replicates for each condition) across all chromosomes for T47D cells grown in the absence or presence of serum. Yellow represents switches to A compartment and dark purple represents switches to B compartment upon serum deprivation. Black horizontal bars represent threshold of p-val>0.001. Genomic positions are indicated at the bottom.

(**B**) Barplot representing the total number of TADs for Hi-C experiments in T47D grown in the presence or absence of serum (4 independent replicates for each condition). No significant differences were observed comparing replicates and conditions (Fisher exact test = 0.326).

(**C**) Scatter plot of Pol II gene expression in T47D cells grown in the presence (+S) or absence (–S) of serum (red, up-regulated in +S; blue, down-regulated in +S; grey, no changes). The number of genes up- or down-regulated in the +S condition (-1.5 < FC > 1.5; adjusted p-value < 0.05) is indicated.

(**D**) Boxplot of mRNA expression for T47D cells grown in the presence (+S, red) or absence (–S, grey) of serum for TFIIIC-associated Pol II promoters. A random dataset of the same size has been used as a control (**p-value < 0.001; two-tailed paired *t*-test). Notice that TFIIIC-associated promoters show higher level of expression compared to a random control. No significant changes were detected when the two growth conditions were compared (two-tailed paired *t*-test).

(**E**) CEAS profile of average total Pol II enrichment at TFIIIC-associated promoters for T47D cells grown in the presence (+S, red) or absence (-S, grey) of serum. The graphs are plotted over the TSS of the TFIIIC-associated promoters in the –S condition (plotted is the –log10 of the Poisson p-value). No significant differences were detected (two-tailed paired *t*-test).

(**F**) Box plot of oneD-normalized interaction scores calculated for all the AEs bound by TFIIIC for T47D grown in the presence (+S) or absence (-S) of serum. Note the significant increase in the interaction score (Kolmogorov-Smirnov Test).

(**G**) Sitepro profile of strand-specific tRNA expression in T47D in conditions of siCTRL or siGTF3C5 in the absence of serum across all tDNAs spanning a 400 bp region (±200 bp relative to the tRNA TSS; plotted is the average expression in RPM). Note no differences in the two profiles.

(**H**) Volcano plot comparing mRNA-seq data of siGTF3C5 *vs* siCTRL in T47D grown in the absence of serum (-S) (plotted the –log10 of the adjusted p-value *vs* the -log2 ratio of siGTF3C5 *vs* siCTRL). The genes that scored significant (adjusted p-value < 0.05) are indicated in red (FC > 1.5) and blue (FC < -1.5). *GTF3C5* is found among the most downregulated genes. See Table S2 for more information.

(**I-J**) Scatter plot of gene expression comparing siGTF3C5 (**I**) and siCTRL (**J**) treated cells in the absence of serum *vs* mock-transfected cells in the same growth condition. The number of genes up- or down-regulated (-1.5 < FC > 1.5; adjusted p-value < 0.05) is indicated in red or blue, respectively.

(**K**) Bar plots of GO enrichment (according to DAVID) of TFIIIC-activated genes (genes downregulated in siGTF3C5 cells).

(**L**) FACS cell cycle profile of T47D cells grown in the absence (–S) of serum or transfected with siCTRL or siGT3C5 in the same growth conditions (n = 2 independent experiments). Note that no effect was observed by the siCTRL treatment, but further cell cycle arrest detected in siGTF3C5 cells (*, p-value for squared χ^2 test = 0.00045).

Fig. S5

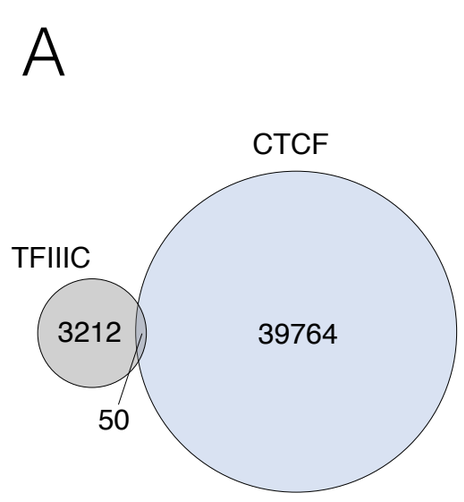
A
CTCF
TFIIIC
3212
39764
50

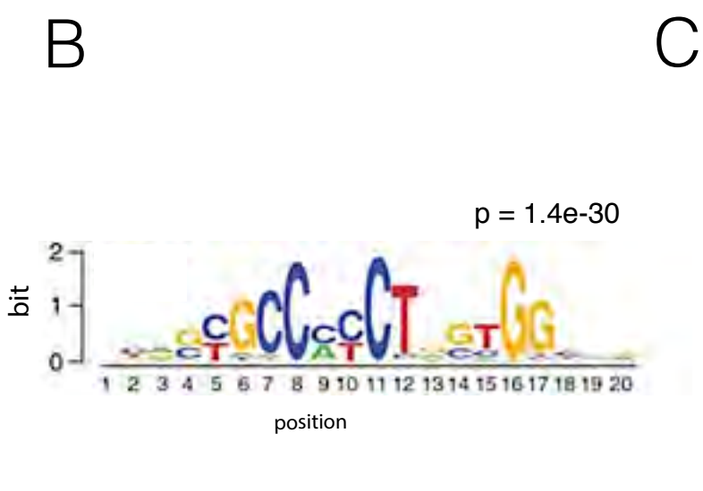
B
p = 1.4e-30
bit
position

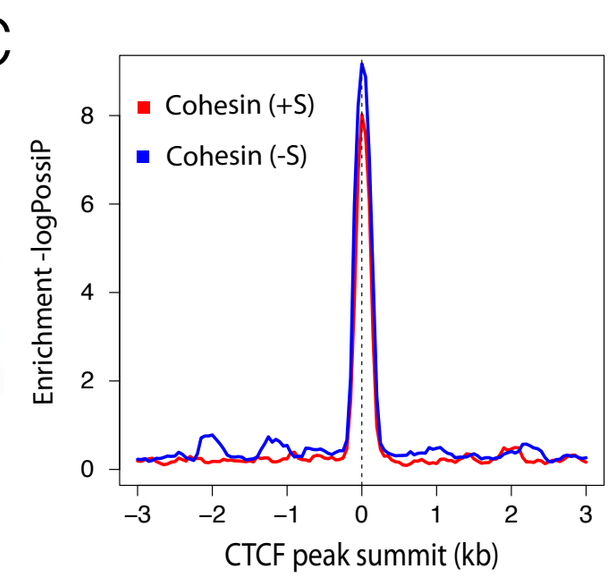
C
Cohesin (+S)
Cohesin (-S)
Enrichment -logPossiP
CTCF peak summit (kb)

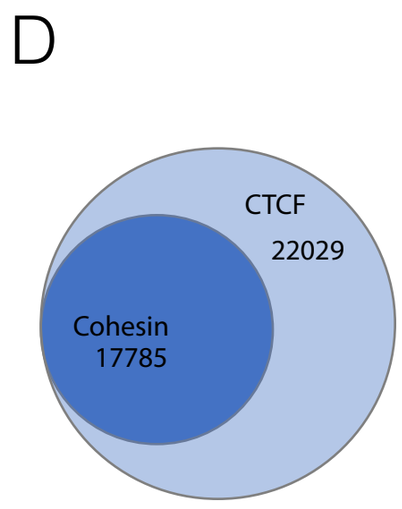
D
CTCF
22029
Cohesin
17785

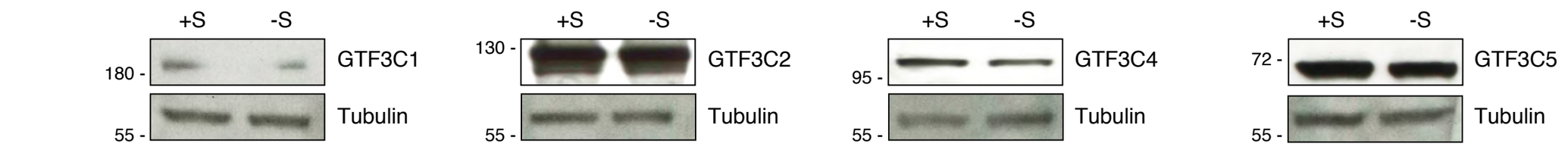
E
+S
-S
180 -
GTF3C1
Tubulin
55 -
130 -
GTF3C2
95 -
GTF3C4
72 -
GTF3C5

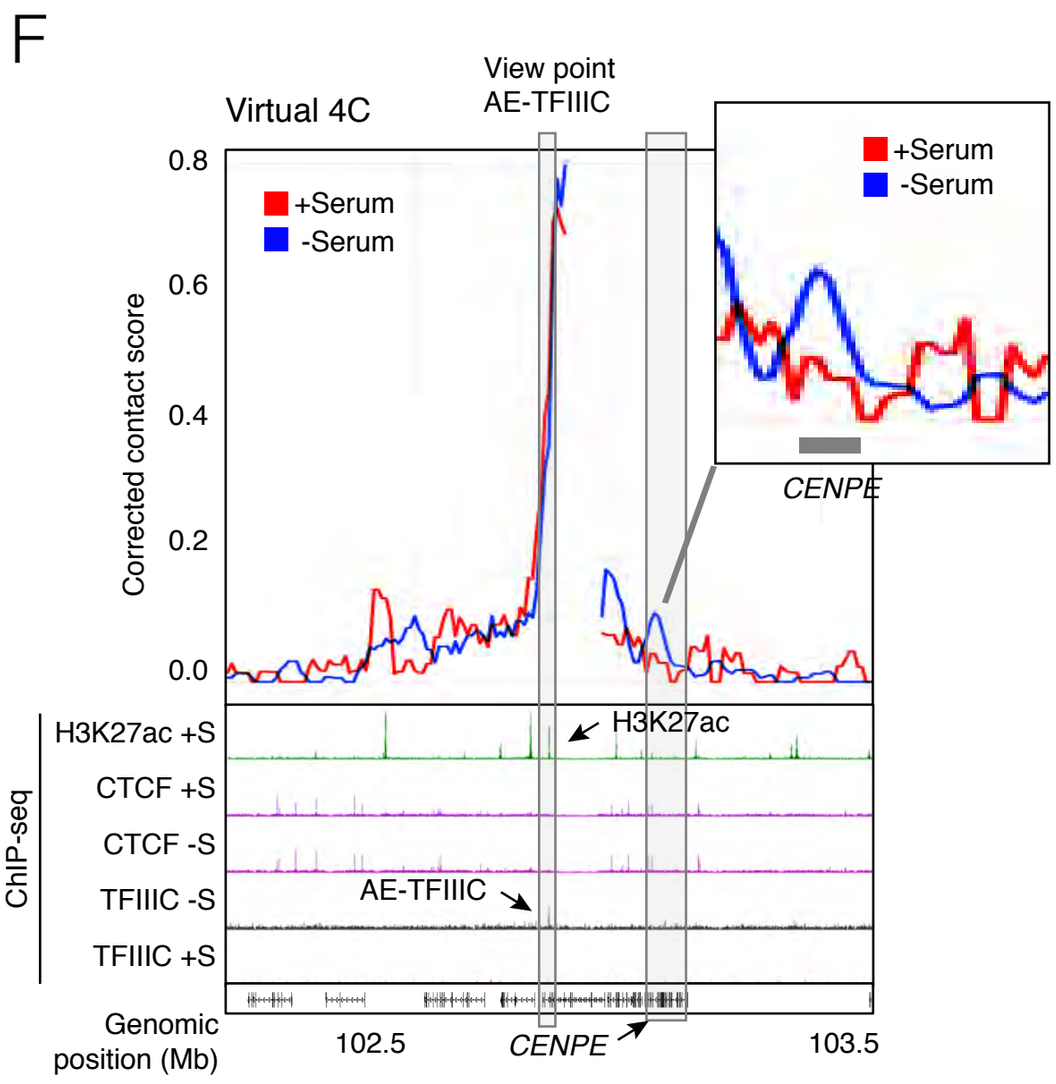
F
Virtual 4C
View point
AE-TFIIIC
+Serum
-Serum
Corrected contact score
CENPE
ChIP-seq
H3K27ac +S
CTCF +S
CTCF -S
TFIIIC -S
TFIIIC +S
H3K27ac
AE-TFIIIC
Genomic
position (Mb)
102.5
103.5

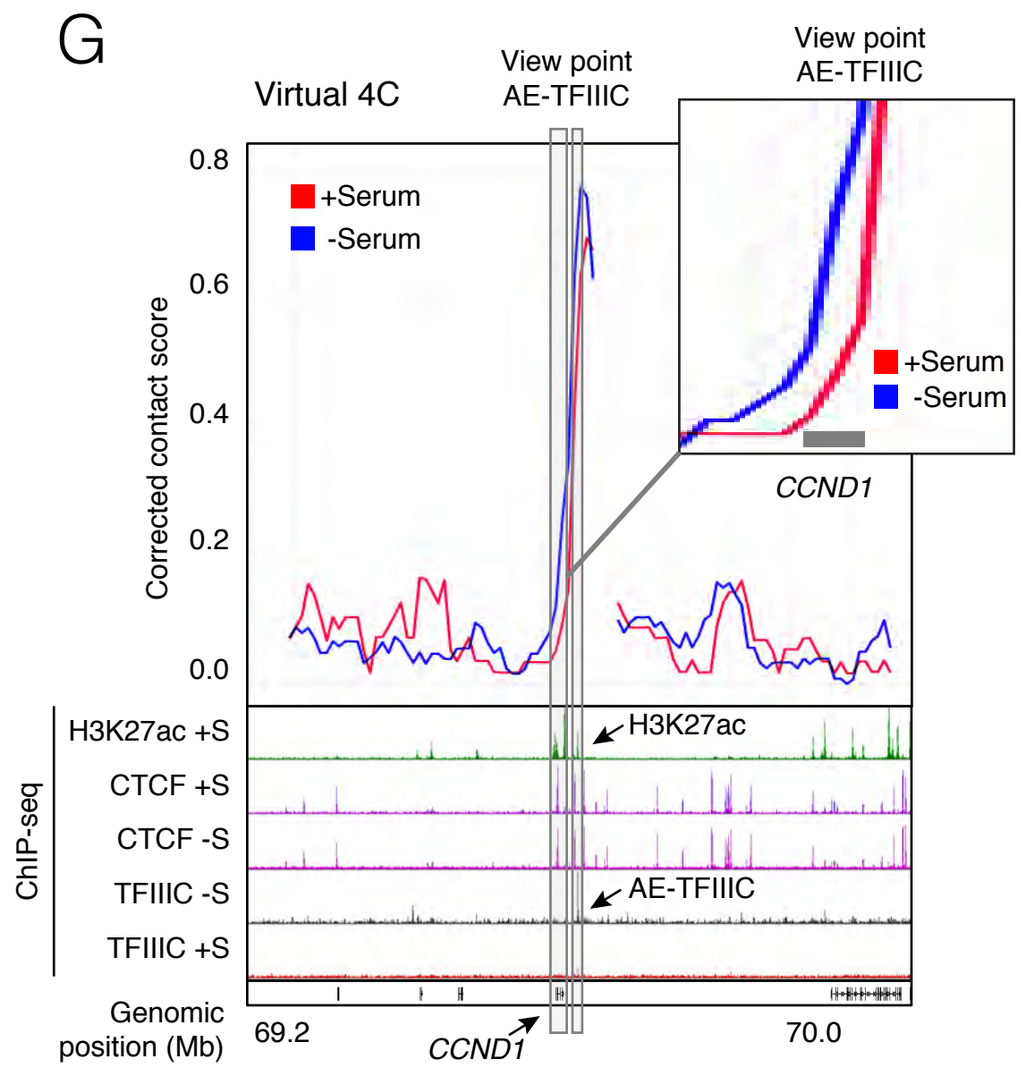
G
Virtual 4C
View point
AE-TFIIIC
+Serum
-Serum
Corrected contact score
CCND1
ChIP-seq
H3K27ac +S
CTCF +S
CTCF -S
TFIIIC -S
TFIIIC +S
H3K27ac
AE-TFIIIC
Genomic
position (Mb)
69.2
70.0

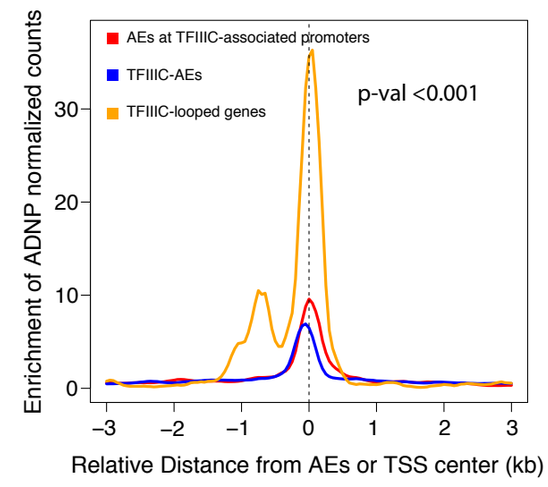
H
AEs at TFIIIC-associated promoters
TFIIIC-AEs
TFIIIC-looped genes
p-val <0.001
Enrichment of ADNP normalized counts
Relative Distance from AEs or TSS center (kb)

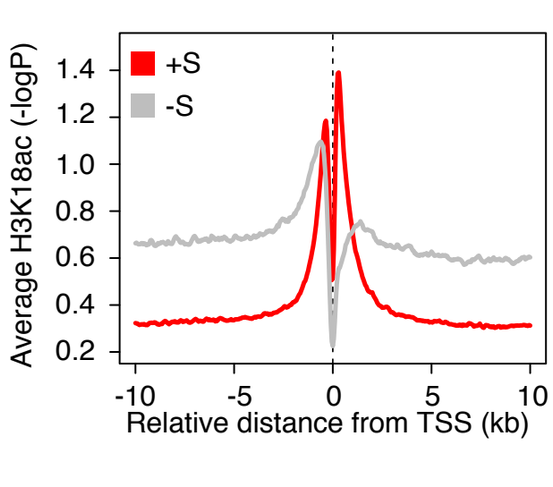
I
+S
-S
Average H3K18ac (-logP)
Relative distance from TSS (kb)

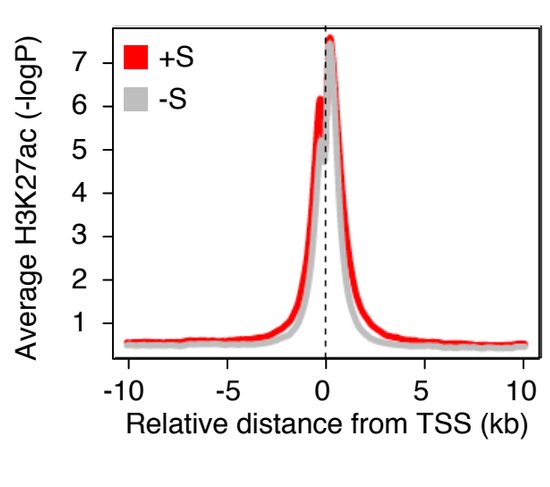
J
+S
-S
Average H3K27ac (-logP)
Relative distance from TSS (kb)

Figure S5. TFIIIC and CTCF increased interaction upon SS does not depend on changes in total levels of TFIIIC, Related to Figure 5.

(A) Venn diagram of overlapping peaks for CTCF and TFIIIC in T47D grown in the absence of serum.

(B) Motif enrichment analysis of CTCF-bound regions in TFIIIC-looped genes. The *p*-value of the motif's enrichment is shown.

(C) Sitepro analysis of RAD21 enrichment at CTCF-bound regions in the TFIIIC-looped genes (red) compared to a random set of regions of the same size (blue). Note that there is no difference in the RAD21 enrichment between the two conditions.

(D) Venn diagram of overlapping peaks for the Cohesin component RAD21 and the CTCF peaks in condition of serum starvation.

(E) Western blot for different TFIIIC subunits (GTF3C1, GTF3C2, GTF3C4 and GTF3C5) in T47D cells grown in the presence (+S) or absence (–S) of serum. For each panel, a loading control with α-tubulin is also shown.

(**F-G**) Virtual 4C (from Hi-C data) representation of the *CENPE* (**F**) and *CCND1* (**G**) loci, two of the genes repressed upon siGTF3C5 (Figure 4C). The data is represented for the conditions of presence (+S red) and absence (–S, blue) of serum. The viewpoint of the virtual 4C is the AE bound by TFIIIC. Arrows point to the location of the gene, the AE bound by TFIIIC (AE-TFIIIC) and the peak of H3K27ac. The y-axis corresponds to the corrected contact score. Regions with changes in the frequency of interaction of the AE-TFIIIC and the target genes have been zoomed out for a clearer view. Grey boxes represent the location of the gene compared to the 4C signal.

(**H**) Sitepro analysis of ADNP-eGFP binding in K562 cells (GSE105573) at AEs of TFIIIC-associated promoters (red), all AEs-bound by TFIIIC (TFIIIC-AEs, blue) and TFIIIC-looped genes (yellow). Significant higher levels of ADNP-eGFP are found at TFIIIC-looped genes (p-values for squared Chi test comparing TFIIIC-looped genes vs AEs at TFIIIC-associated promoters and TFIIIC-AEs is reported). X-axis is either the center of the AE (for the AEs at TFIIIC-associated promoters or TFIIIC-AEs, or the TSS of the TFIIIC looped genes).

(**I-J)** CEAS plot of H3K18ac (**I**) and H3K27ac (**J**) average at the TSS of all human genes in T47D grown in the presence (+S, red) or absence (–S, grey) of serum (plotted is the –log10 of the Poisson p-value). Note how H3K18ac drastically changed upon serum starvation, whereas H3K27ac remained unaffected.

Fig. S6

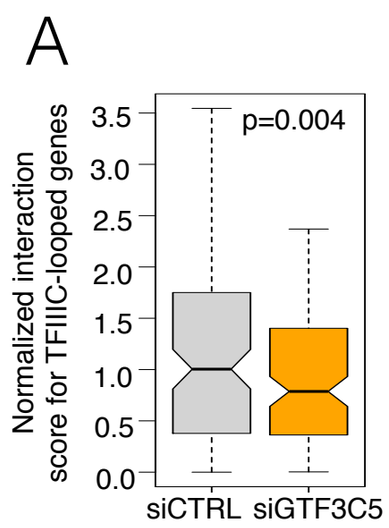
A
Normalized interaction score for TFIIIC-looped genes
3.5
3.0
2.5
2.0
1.5
1.0
0.5
0.0
p=0.004
siCTRL
siGTF3C5

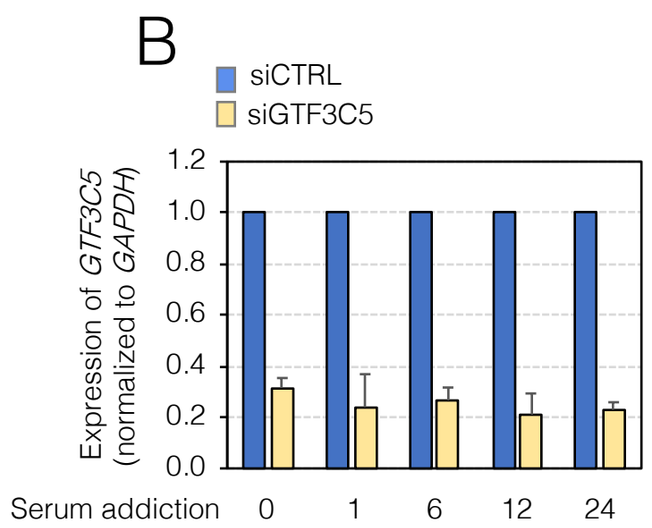
B
siCTRL
siGTF3C5
Expression of GTF3C5 (normalized to GAPDH)
1.2
1.0
0.8
0.6
0.4
0.2
0.0
Serum addiction (h)
0
1
6
12
24
Time

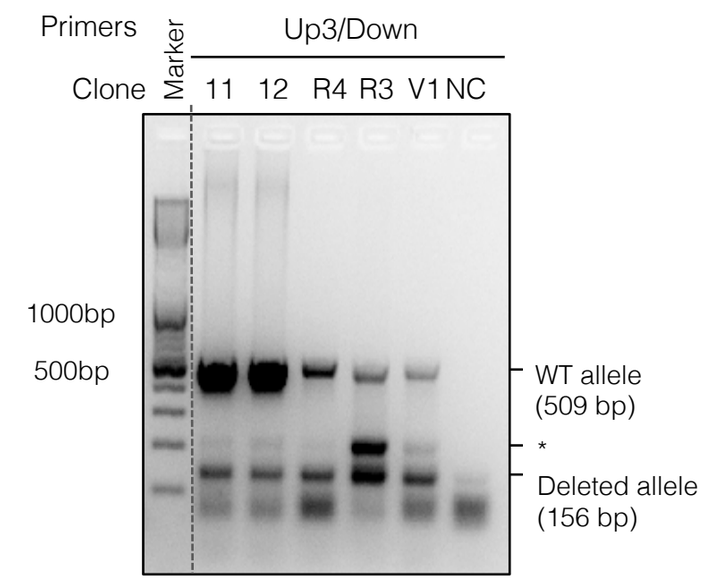
C
Primers
Up3/Down
Clone
Marker
11
12
R4
R3
V1
NC
1000bp
500bp
WT allele (509 bp)
*
Deleted allele (156 bp)

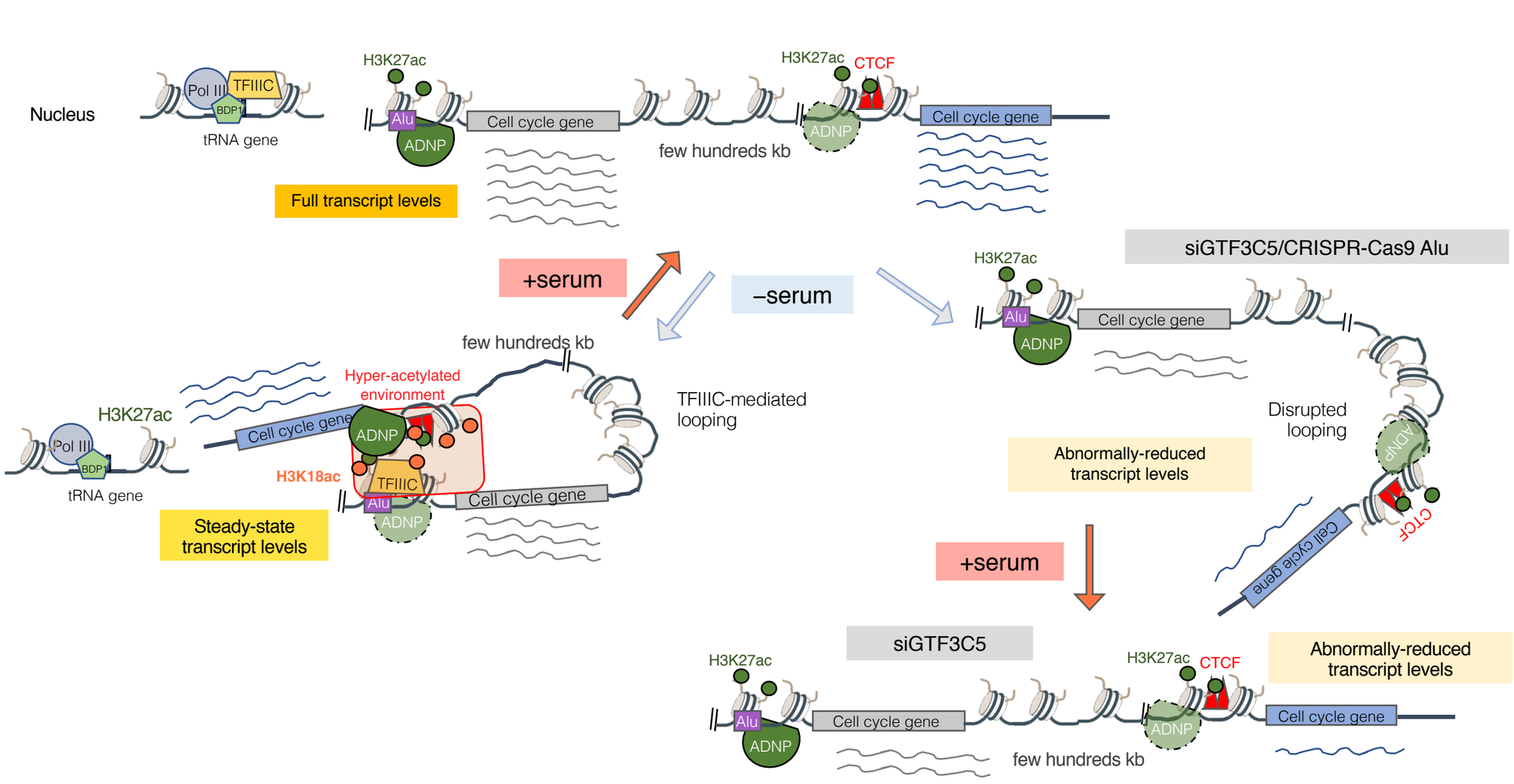
D
Nucleus
Pol III
TFIIIC
BDP1
tRNA gene
H3K27ac
Alu
ADNP
Cell cycle gene
few hundreds kb
CTCF
Full transcript levels
+serum
–serum
siGTF3C5/CRISPR-Cas9 Alu
Hyper-acetylated environment
H3K18ac
TFIIIC
TFIIIC-mediated looping
Steady-state transcript levels
Disrupted looping
Abnormally-reduced transcript levels
siGTF3C5

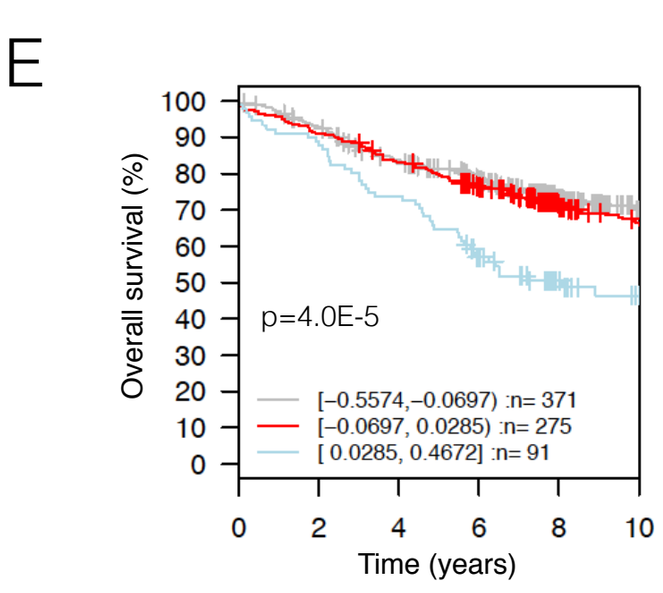
E
Overall survival (%)
100
90
80
70
60
50
40
30
20
10
0
p=4.0E-5
[–0.5574,–0.0697) :n= 371
[–0.0697, 0.0285) :n= 275
[0.0285, 0.4672] :n= 91
0
2
4
6
8
10
Time (years)

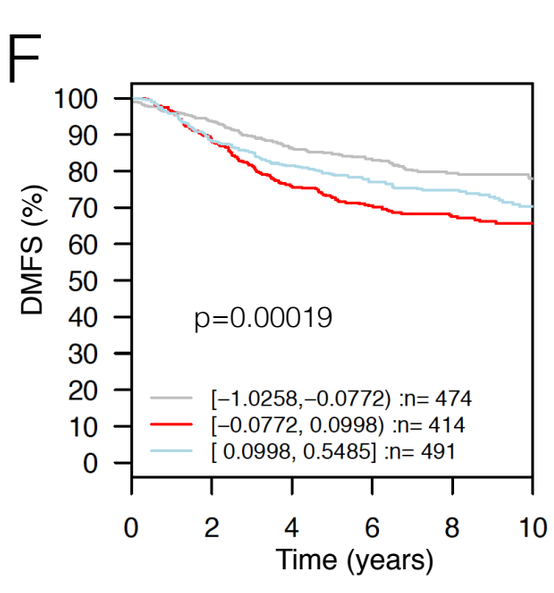
F
DMFS (%)
100
90
80
70
60
50
40
30
20
10
0
p=0.00019
[–1.0258,–0.0772) :n= 474
[–0.0772, 0.0998) :n= 414
[0.0998, 0.5485] :n= 491
0
2
4
6
8
10
Time (years)

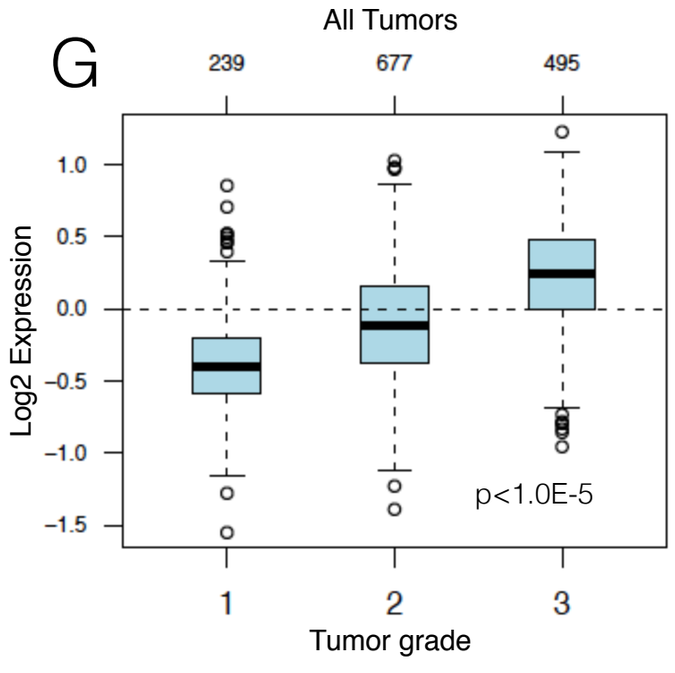
All Tumors
G
239
677
495
Log2 Expression
1.0
0.5
0.0
–0.5
–1.0
–1.5
p<1.0E-5
1
2
3
Tumor grade

Figure S6. The deletion of a TFIIIC-bound AE affects DNA looping and expression of the distal *UHRF1* locus, Related to Figure 6.

(**A**) Boxplot of the normalized interaction score of Hi-C data for siCTRL and siGTF3C5 between promoters and TFIIIC-bound AEs for TFIIIC-looped genes. Two Hi-C biological replicates were used (p-value from Friedman X^2 test is indicated).

(**B**) qRT-PCR expression analysis of *GTF3C5* in T47D cells treated with siCTRL and siGT3C5 in the absence of serum and released from serum starvation by serum addition for the indicated times. Samples correspond to Figure 6D. The graph represents the mean ± SEM from two biological experiments, in which the value in siCTRL cells was arbitrarily set as 1 at each time point. Note that the knockdown of TFIIIC always reaches values of more than 70% at each time point analyzed.

(**C**) PCR result for the screen of CRISPR-Cas9 T47D clones with primers Up3 and Down (see Supplementary Materials and Methods for details and schematic representation in Figure 6E): the upper band corresponds to the WT allele, whereas the lower band correspond to the deleted allele. Representative clones are shown, but almost all clones analyzed were heterozygous for the deletion. For further analysis, clone 11 was selected. The DNA marker size is shown. * indicates a non-specific band. NC corresponds to no DNA sample. Dotted line represents a cut of the gel. However, all the remaining lanes are from the same gel.

(D) Cartoon model for the proposed TFIIIC mechanism of action.

(**E-F**) Kaplan–Meier plots of breast tumor samples for TFIIIC-associated promoters or TFIIIC-activated genes expression, respectively. TFIIIC-associated promoters were divided in three main groups according to their expression levels within brackets (with blue being the highest, red the intermediate and grey the lowest). P-values from a Mantel-Cox test are indicated. Higher expression of TFIIIC-associated promoters is associated with poor prognosis for overall survival and distance metastasis free survival (DMFS), respectively. Plots are generated using (GOBO) (Ringner et al., 2011).

(**G**) Boxplots of expression of TFIIIC-associated promoters from all tumor samples across the three breast cancer grades. Box plots are generated by using (GOBO). TFIIIC-associated promoters show higher expression in most aggressive tumors (3rd grade), p-value is also indicated.